Particulate number emissions during cold-start with diesel and biofuels: A special focus on particle size distribution

Ali Zare[a,*], Timothy A. Bodisco[a], Puneet Verma[b,c], Mohammad Jafari[b,c], Meisam Babaie[d], Liping Yang[e], M.M Rahman[f], Andrew P.W. Banks[g], Zoran D. Ristovski[b,c], Richard J. Brown[b], Svetlana Stevanovic[a]

[a] School of Engineering, Deakin University, VIC, 3216 Australia

[b] Biofuel Engine Research Facility, Queensland University of Technology (QUT), QLD, 4000 Australia

[c] International Laboratory for Air Quality and Health, Queensland University of Technology (QUT), QLD, 4000 Australia

[d] School of Computing, Science and Engineering (CSE), University of Salford, Salford, Manchester M5 4WT, United Kingdom

[e] Institute of Power and Energy Engineering, Harbin Engineering University, No. 145-1, Nantong Street, Nangang District, Harbin, 150001, China

[f] School of Mechanical Aerospace and Automotive Engineering, Coventry University, Coventry CV1 2JH, UK

[g] Queensland Alliance for Environmental Health Sciences, The University of Queensland, , QLD, 4072 Australia

[*] Corresponding author: Ali Zare, ali_z4688@yahoo.com, ali.zare@deakin.edu.au

Abstract

The share of biofuels in the transportation sector is increasing. Previous studies revealed that the use of biofuels decreases the size of particles (which is linked to an increase in particulate toxicity). Current emission regulations do not consider small particles (sub-23 nm); however, there is a focus in future emissions regulations on small particles. These and the fact that within cold-start emissions are higher than during the warmed-up operation highlight the importance of a research that studies particulate matter emissions during cold-start. This research investigates the influence of biofuel on PN and PM concentration, size distribution, median diameter and cumulative share at different size ranges (including sub-23 nm and nucleation mode) during cold-start and warm-up operations using diesel and 10, 15 and 20% mixture (coconut biofuel blended with diesel). During cold-start, between 19 to 29% of total PN and less than 0.8% of total PM were related to the nucleation mode (sub-50 nm). Out of that, the share of sub-23 nm was up to 9% for PN while less than 0.02% for PM. By using biofuel, PN increased between 27 to 57% at cold-start; while, the increase was between 4 to 19% during hot-operation. The median diameter also decreased at cold-start and the nucleation mode particles (including sub-23 nm particles) significantly increased. This is an important observation because using biofuel can have a more adverse impact within cold-start period which is inevitable in most vehicles' daily driving schedules.

Keywords: Particle size distribution; PN; sub-23 nm; biofuel; cold-start.

Word count: 7338

Abbreviations	
NOx	Nitrogen oxides
CO	Carbon Monoxide
HC	Hydrocarbon
PM	Particle mass
PN	Particle number
BSFC	Brake Specific Fuel Consumption
CMD	Count median diameter
ECU	Engine control unit
EU	European Union
VOCs	Volatile organic compounds

Highlights

1. This study investigated engine-out particle emissions and size distribution
2. Cold-start, hot-start, and two intermediate warm-up phases were studied
3. Nucleation mode particles increased as the engine warmed up
4. During cold-start, using biofuel decreased the size of particles
5. Sub-23 nm fraction contributed up to 0.02% and 9% to cumulative PM and PN

1. Introduction

The transportation sector has been undergoing a significant transformation with the utilisation of different strategies and technologies to reduce harmful emissions [1]. One of these strategies is related to fuel. The adverse effect of using fossil fuels in the transportation sector has created significant interest in renewable alternatives, such as biofuels. There have been incentives in place to increase the share of such renewable alternatives. For example, EC Directive 2003/30 was issued to increase the share of biofuel to 5.75% by 2010 and Directive 2009/28/EC targeted a share increase to 10% by 2020. One of the reasons for increasing the share of renewable fuel in the transportation sector can be the advantages it has on engine performance and exhaust emissions [2-4].

In terms of engine performance parameters, it has been reported that using biofuels (such as jatropha biodiesel) can improve the thermal efficiency of diesel engines when compared to diesel fuel; however, it depends on the type of biofuel [5-7]. Friction parameters were also reported to be lower with biodiesel owing to their better lubricity [8, 9]. However, fuel consumption parameters such as brake specific fuel consumption (BSFC) were reported to be higher and the engine power was reported to be lower with biofuel derived blends [10, 11]. The higher viscosity, higher density and lower calorific values of biofuels were reported to be primary reasons. In terms of emissions, lower hydrocarbon (HC) and carbon monoxide (CO) emissions were reported to be advantages of using biofuels [12-14]. However, it has been frequently reported that nitrogen oxides (NOx) emissions increase with biofuels (some articles claimed otherwise) [15-17]. Maybe the most highlighted advantage of using biofuel is the decrease in particulate matter emissions; however, some articles reported a different observation [18, 19]. It has been frequently reported that particulate matter emissions decrease significantly due to the oxygen content of the biofuel [18, 20, 21].

Particulate matter emissions can adversely affect our environment and are identified as a global risk factor as these emissions have been reported to be associated with cardiorespiratory health problems [22-24]. It was shown that prolonged exposure to particulate matter emissions is associated with an increase in free-radicals which adversely impact health [25-27]. Particulate matter emissions can be evaluated from two inter-correlated perspectives. The first aspect is the particulate mass (PM) which reports the mass of particles. However, this measurement might not be able to provide sufficient information when it comes to the health hazards from particles, as those very small particles which are harmful have a lower contribution to PM [28]. However, the second perspective, particulate number (PN), is more informative and has gained a lot of attention, therefore it became mandated in the recent emissions regulations [29]. For passenger cars, reporting PN emissions became mandated from the Euro 5 emissions regulation [29], while there was no regulation on PN in Euro 1-4 [29]. The PN, which is the count of individual particles can include small particles even those with nearly zero weight and contribution to PM.

Using biofuel has been reported to have different effects on PN emissions, some reported higher PN with biofuels and some reported lower [18, 30]. However, most of the reports in the literature showed that using biofuel decreases the size of particles [31, 32]. This is important as it has been reported that a decrease in particle size is associated with an increase in toxicity [33]. However, in the most recent emission regulations such as Euro 5 and 6 and WLTP (worldwide harmonised light vehicles test procedure), there is a guideline for PN measurement—PMP (particle measuring method)—which does not consider sub-23 nm particles [34-36]. PMP does specify the count efficiency of 50% (D_{50}) at 23 nm and 90% (D_{90}) at 41 nm, and it has been reported in the literature that decreasing D50 from 23 nm to smaller sizes such as 10 nm can significantly increase the PN emissions from vehicles [37, 38]. For example, Leach et al. [38] reported that decreasing D_{50} and D_{90} to 10 nm and 23 nm leads to 36% higher PN. This and the increasing share of biofuel in the transportation sector highlight the importance of studying PN emissions in more detail such as looking into the size of particles.

PN emissions from an engine depend on different factors such as operating conditions [39]. For a high portion of vehicles, the cold-start operation is a norm which occurs mostly in the morning and afternoon when people start their vehicle after some hours of engine-off and drive between home and work. It has been reported that a significant number of trips between home and work start and finish during the cold-start period [40]. For example, a study of more than one thousand trips showed that more than 30% of the trips started and finished within the cold-start period [41]. Regulation (EU Directive 2012/46/EU) considers the cold-start period from engine start—after 12 hours soak (or 6 hours forced cooled)—either for the first 5 minutes or during the time that the temperature of engine coolant increases to 70°C. Within this period, the engine temperature is sub-optimal affecting the combustion process [42]. Consequently, engine emissions and performance are different in comparison with hot-operation [43-45]. For example, fuel consumption and friction power were reported to be higher when the engine is cold [46]. This was reported to be because of the high viscosity of the engine oil at lower temperatures, which consequently leads to higher friction, therefore more fuel needs to be burnt to maintain power [40, 46]. Fuel evaporation and atomisation are also impacted by the lower temperature of the engine and fuel during cold-start which also impacts emission and performance parameters [18].

It has been reported that during cold-start, emissions are higher than when the engine is fully warmed up [47, 48]. For example, a study used a custom driving cycle and showed that during the cold-start period of the cycle, PN emissions with biofuel increased significantly compared to the hot-operation period [47]. Another study showed that around one-third of the emitted PM emissions were related to the first 12% of the total distance (Phase 1) of the LA92 Unified Driving Cycle [49]. It also reported that compared to Phase 3 of that cycle, in which the engine was fully warmed up, during Phase 1, which was cold-start, the PM emissions were 7.5 times higher. Some studies in the literature investigated other emissions such as CO, CO_2 and NOx [40, 50, 51]. However, there are a few studies that investigated PN emissions and size distribution during cold-start in detail, when compared to other emissions [52]. Also, most of the cold-start experimental studies in the literature used driving cycles such as NEDC (New European Driving Cycle) or WLTC (worldwide harmonised light vehicles test cycle) which has abrupt load/speed changes. The results of such studies were shown with the averaged value. However, it is essential to study the influence of transient engine temperature while the engine is warming up on exhaust emissions such as PN. It will be seen in this current study that cold-start and engine warm-up have different stages and therefore different impacts on exhaust emissions.

This research aims to study the influence of fuel and transient engine temperature at different stages of engine warm-up (including cold-start) on particulate matter emissions from different aspects including PN, PN and PM size distribution and median diameter, the share of particles at different sizes, nucleation mode particles and sub-23 nm particles. The increasing share of biofuels in the market, with the inherent decrease in particle size and the associated increase in toxicity, increased emissions during cold-start coupled to future emissions regulations on small particles, and the fact that the current emission regulations do not consider sub-23 nm particles, all highlight the importance of this study. By using and comparing different biofuel blending ratios (10, 15 and 20%), this study can be helpful to engine researchers when it comes to nucleation mode and sub-23 nm particles the upcoming emissions regulations.

2. Methodology

The engine used in this study was a Cummins ISBe220 diesel engine (designed and manufactured by an American company) which is an in-line 6-cylinder, turbocharged, common-rail engine, as shown in Table 1. The maximum torque and power with this engine are 820 Nm (at 1500 rpm) and 162 kW (at 2500 rpm) and the engine was coupled to an in-house hydraulic dynamometer (electronically-controlled). The experiments were done at QUT Biofuel Engine Research Facility (BERF) in Brisbane, Australia.

Table 1 Engine specifications

Model	**Cummins ISBe220 31**
Aspiration	Turbocharged
Fuel injection	Common rail
Cylinders	6 in-line
Capacity	5.9 L
Bore × stroke	102 × 120 (mm)
Maximum torque	820 @ 1500 (Nm @ rpm)
Maximum power	162 @ 2500 (kW @ rpm)
Compression ratio	17.3:1

Figure 1 shows a schematic diagram of the experiment setup. Engine and dynamometer data were collected with Dynolog software. The in-cylinder data such as crank angle and injection signals were collected using a Kistler (6053CC60) transducer, Kistler type 2614 sensor and DT9832 A-to-D convertor, which all were connected to an in-house National Instruments

LabView program [53, 54]. The accuracy of the measuring instruments are shown in Appendix (Table A1).

To better evaluate the pure effect of fuel properties and also the engine temperature, this study evaluated the engine-out emissions instead of tailpipe emissions (which are sampled before any after-treatment system). This way the emissions do not depend on the after-treatment systems performance/type. Therefore, the fundamental study will not be limited and results can give more information about the real engine dependent emission [55]. In order to measure particulate matter emissions (such as particle number, mass, size distribution), this study used a TSI scanning mobility particle sizer (SMPS) consisting of a TSI 3071A classifier (which preselects the particles in different sizes) and a TSI 3782 CPC (which grows the particles to make them detectable for the optic). SMPS is designed and manufactured by TSI which is an American company. SMPS has a size resolution capability of 128 channels per decade, which results in 192 channels in total. The exhaust gas (which had a temperature of ~350 °C) was directed to the SMPS, but after being diluted (~20 times) with ambient air (~23 °C) which was passed through a HEPA filter in a constant volume dilution system (CVS). The CVS setup was followed by the European legislation (Commission Regulation (EU) 2017/2400). To calculate the dilution ratio, a CAI-600 and a SABLE CA-10 CO_2 analysers (designed and manufactured by American companies) were used before and after the dilution system measuring the CO_2 emissions.

The exhaust particles are made of solid particles, volatiles and liquid droplets. Usually, the PMP method uses a volatile particle remover (VPR) system including three stages of hot dilution (PND_1), heated evaporative tube (ET) and cold dilution (PND_2) to minimise the effect of volatiles and liquid droplets ensuring that the particle counter measures solid particles

(ECE/TRANS/WP.29/GRPE/2016/3 amended by GRPE-72-09-Rev.2) [56]. Regarding the difficulty of sub-23 nm measurement with current instruments in the market [36], it is worth mentioning that SMPS is capable to measure particles above 10 nm including solid particles and volatiles.

This study reports PN and PM, and also PN and PM size distribution. Regarding the PN and PM size distribution, SMPS measures the number of concentration in a given channel (dN) and divides it by the geometric width of the size of channel, and reports the normalised number concentration ($dN/dlogD_p$), where D_p is the geometric midpoint of the particle size channel. The conversion of PN to PM was done through the Aerosol Instrument Manager Software for SMPS Spectrometer using the formula $dM = dN \cdot (\pi/6)D_p^3\, \rho$, where ρ is density, and reporting the normalised mass concentration using the formula $dM/dlogD_p = dN/dlogD_p \cdot (\pi/6)\, D_p^3\, \rho$ [57]. In general, based on the size distribution, the measured ultrafine particles can be classified into two modes; nucleation mode and accumulation mode [28]. The nucleation mode particles are defined as particles with diameters less than 50 nm, and the size of accumulation mode particles is between 50-500 nanometres, and these definitions are used in this study to better interpret the data [28].

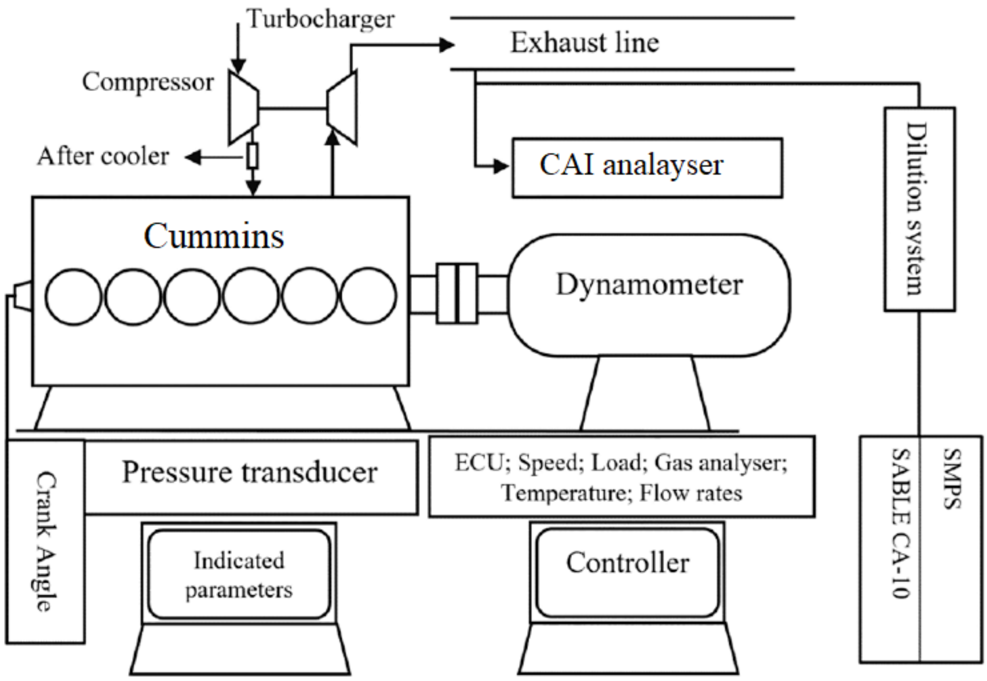

Figure 1 Test setup schematic diagram

Given that this study intended to investigate particulate matter emissions based on the current and future emissions regulation requirements, the selection of the fuels was conducted in a way to cover past, current and future biofuel blending ratio in the market. Therefore, it used diesel, and then made three diesel/biofuel blends of 10, 15 and 20% (by volume) denoted as D90C10, D85C15 and D80C20 using coconut oil biofuel (this study is a part of a project which investigates the potential of using different biofuels in diesel engines in Marshal Islands which have a high resource of coconut). In the tested fuel names, D stands of diesel and the digits after that show the volume of diesel in the blend. And C stands for coconut biofuel and the two digits after C shows the blending ratio. These fuel blends will be evaluated against diesel (D100).

Table 2 shows the tested fuel properties and Table 3 shows the chemical composition of fuels analysed by a GC/MS instrument (Trace 1310 Gas chromatograph, model ISQ, single quadrupole MS). Diesel (D100) contained aromatic compounds (benzene and its derivates, naphthalene, xylene, phthalan, mesitylene) and aliphatic compounds (mainly alkanes with 7-13 carbons, low concentrations of limonene). D90C10, D85C15, and D80C20 also contained cycloalkanes, cyclohexane and cyclooctane. With D100, the aromatic content was higher compared to other fuels. Compared to neat diesel, fuels with a lower blending ratio do not change the fuel properties significantly. For example, the density of the tested fuels, D100, D90C10, D85C15 and D80C20 were 0.84, 0.843, 0.845 and 0.846 g/cc. Also, the lower heating value of the tested fuels, D100, D90C10, D85C15 and D80C20 were 41.77, 41.31, 41.09 and 40.86 MJ/kg, respectively. However, even small changes in fuel properties can affect engine performance and emissions. For example, the higher density and lower calorific value of biofuel blends can negatively impact engine power and also fuel consumption parameters such as BSFC [8]. The fuel oxygen content of biofuel is another property that distinguishes biofuel from diesel (which has no oxygen content). It has been frequently reported that fuel oxygen content is the primary driver for decreased PM emissions with biofuels [18, 19, 58].

Table 2 Fuel properties

	D100	C100	D90C10	D85C15	D80C20
Density at 15 ºC (g/cc)	0.84	0.87	0.84	0.84	0.85
Kinematic viscosity at 40 °C (mm^2/s)	2.64	4.82	2.86	2.97	3.08
Cetane number	53.30	58.60	53.83	54.10	54.36
Lower heating value (MJ/kg)	41.77	37.20	41.31	41.08	40.86
Higher heating value (MJ/kg)	44.79	39.90	44.30	44.06	43.81

Table 3 Fuel analysis using GC/MS (Model ISQ, single quadrupole MS, Trace 1310 Gas chromatograph).

	Area %				
	aromatic	aliphatic	cyclic hydrocarbons	hydrazide	oxygenated hydrocarbons
D90C10	0.0879-0.169	0.0866-0.367	0.119-1.12	1.09-2.62	0.192-0.305
D80C20	0.0433-0.0968	0.0398-0.741	0.0394-0.222		0.0416-0.076
D100	1.43-5.66	1-12.24			

The fuels used in this study were tested under constant load (25%) and speed (1500 rpm). The rationale for using a constant load and speed was to facilitate the fundamental investigation into the influence of fuel type & engine temperature under cold-start and during engine warm-up. Most of the studies on cold-start in the literature used a drive cycle such as NEDC or WLTC and compared the first part of the cycle with the rest and made the conclusion about cold-start contribution. However, these driving cycles consist of frequent load and speed changes which add more variables to the analysis, complicating and limiting the investigation about the pure influence of fuel type and engine temperature on emissions within cold-start period. Therefore, this experimental investigation used a constant speed and engine load to limit the number of influential factors that can potentially aid a better judgment on the effects of engine temperature and fuel properties.

Experiments were done every morning with at least 12-hours of engine-off period at the ambient temperature on consecutive days in an engine laboratory. Before starting each test, coolant temperature and lubricating oil temperature were checked to be the same as ambient temperature, as per the regulation (EU Directive 2012/46/EU). Given that the engine room had an air-conditioning system, the ambient temperature during the test stayed constant (23±5 °C). For each test, the engine was started and ran under a quarter load (25%) at the speed of 1500 rpm for more than 30 min to stabilise. The statistical analysis of the test repeatability is shown in Appendix.

In diesel engines, the formation of particulate matter emissions depends on a number of variables such as engine operating condition and fuel properties [18]. During cold-start operation, the engine temperature and fuel properties are significantly influential factors. Figure 2 shows how the engine coolant temperature increases during cold-start operation with the tested engine for one of the tests. According to the regulation, (EU Directive 2012/46/EU), the cold-start period is defined from when the engine starts after 12 hours soak (or 6 hours forced cooled soak) at the ambient condition either for the first 5 minutes or during the time that the temperature of engine coolant increases to 70°C. However, after this period, the coolant temperature still has an increasing trend indicating the sub-optimal engine temperature (Figure 2). Also, it can be seen that there is a lag between the engine lubricating oil temperature and coolant temperature. Compared to the coolant temperature, the engine lubricating oil temperature remains sub-optimal for a longer period). The sub-optimal temperature period outside the formal cold-start boundaries can affect the engine performance and exhaust emissions [59, 60]. Figure 2 also shows that for the tested engine, even within the formal cold-start period, when the engine temperature reaches to 65°C, the start of injection is changed by the injection strategy commanded by the ECU of the tested engine, and this injection strategy change affects the exhaust emissions and engine performance parameters. It is worth mentioning that while the start of injection changed, the injection period (therefore, the injection mass) remained constant, as the injection was controlled by the ECU and, the injection period was independent of the start of injection. Also, there was no modification to the engine ECU/calibration for different fuel blends. Therefore the start of injection timing stayed the same for all the tests.

As discussed, it can be seen that from the engine start until the stable operation, there are some periods with different characteristics and variables. Therefore, in order to better analyse the influence of fuel properties and engine temperature, this research divides the engine warm-up period into four phases to minimise the number of variables in each phase.

- Phase 1: Formal engine cold-start, constant start of injection, coolant and oil temperatures are less than 65°C.
- Phase 2: Start of injection is increasing, coolant and oil temperatures above 65°C and still increasing.
- Phase 3: Constant start of injection, optimal coolant temperature, sub-optimal oil temperatures.
- Phase 4: Engine hot-operation, start of injection is constant, coolant and oil temperatures are optimal.

This study used an SMPS analyser with a 2 min sampling time. The first two samples were measured within Phase 1, the third sample was measured in Phase 2, the fourth and fifth samples fell into Phase 3, and the last two samples were measured within Phase 4.

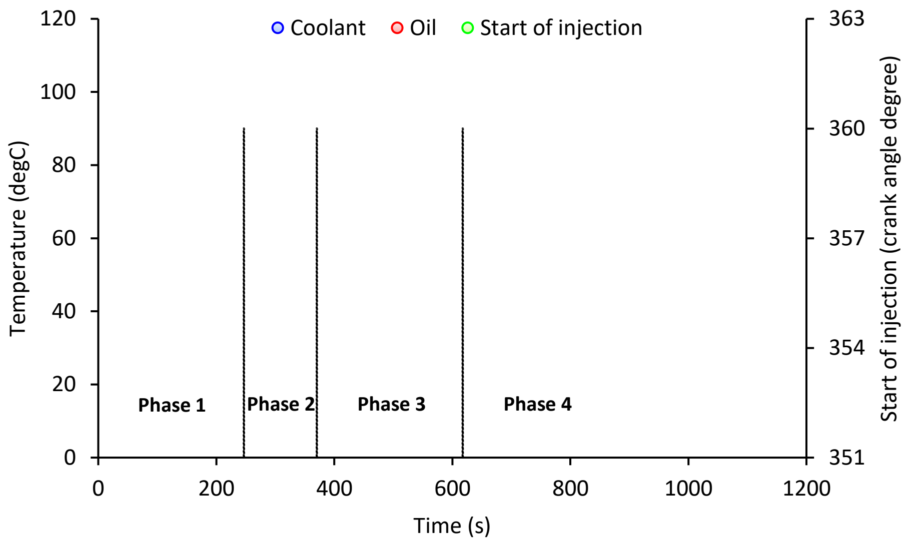

Figure 2 Engine coolant temperature, engine oil temperature and start of injection during the test with diesel

3. Result and discussion

This section analyses the PN concentration and evaluates the particle number and mass size distribution. It also investigates the median diameter and the share of PN and PM at different sizes including accumulation mode, nucleation mode and sub-23 nm particles.

Figure 3 presents the PN concentration at the four different phases. It shows that for each fuel the PN concentration in Phase 1 was lower than the other phases. Given that the engine load and speed were constant within all phases, the engine temperature can be identified as an influential factor, as shown in the literature [61]. Looking at each phase, it can be seen that the use of biofuel increased PN emissions in all of the phases. This expected result shows that fuel properties are influential, as reported before in the literature [62, 63].

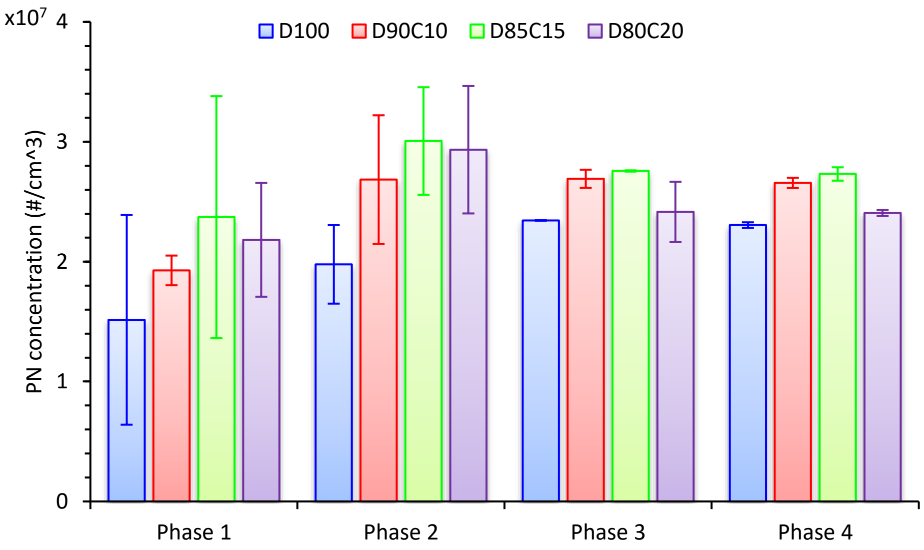

Figure 3 PN concentration at different phases with all the tested fuels

When it comes to the potential health impact of particles, PN can also be analysed in more detail by looking into the size distribution of particles [28, 33]. Reported hypotheses mentioned that when compared to bigger particles, small particles penetrate in lungs deeper and their relatively larger surface area increases the reaction with lung cells; a decrease in the size of particles is also associated with an increase in toxicity [33]. Figure 4 shows the median diameter of the particles with all the tested fuels at different phases. It can be seen that the size of the particles changes as the engine warms up. From Phase 2 to Phase 4, it can be seen that as the engine warms up, the size of particles slightly decreases [64].

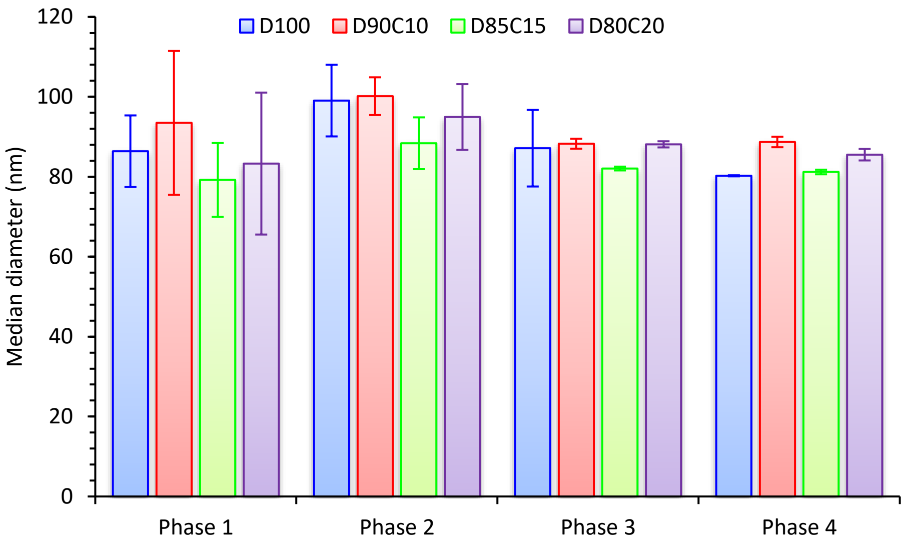

Figure 4 PN median diameter at different phases with all the tested fuels

As discussed, cold-start operation and fuel properties are two factors that can significantly affect the PN concentration and particle size, shown in the literature as well [47]. Therefore, the following analysis is divided into two parts. It first analyses the data from the engine temperature and cold-start perspective and then discusses the influence of fuel properties.

3.1 Influence of engine temperature

Figure 5 shows the variation of PN concentration at the different phases as compared to Phase 1 (cold-start). It can be seen that the PN concentration was higher at other phases when compared to Phase 1. As a constant engine load/speed was maintained through all of the phases, the engine temperature can be considered as the driving factor for any change [52]. In Figure 5, the exhaust temperature is used as an indicator of the engine temperature at the different phases. It can be seen that the exhaust temperature increased from Phase 1 to Phase 4, however, the change between Phases 3 and 4 was not as significant as between Phases 1 and 2. The reason for using the exhaust temperature as an indicator instead of coolant temperature, was that when the coolant temperature reaches to an optimum level, the engine is still warming up.

Phase 1, which had the lowest PN, falls into the cold-start period. As per the regulation, EU Directive 2012/46/EU, the cold-start period can last 5 min from the engine start or until the engine coolant temperature reaches 70°C. During Phase 1, the engine coolant temperature was less than 70°C. Also, during this phase, the start of injection did not change as the engine coolant temperature was less than 65°C, which is the threshold for the injection strategy of the tested Cummins engine.

During Phase 2, the PN concentration was significantly higher than Phase 1. This increase was between 27 to 39%. For example, with neat diesel, D100, the PN concentration increased by 31%, with D80C20 the PN concentration increased by 39%. The significant change between Phases 1 and 2 is a combination of the increase in engine temperature and the injection strategy change, with the latter being assumed as the dominant driver. During this unsteady phase, coolant temperature increased to 65°C and the start of injection changed significantly as by the ECU. This significant increase in the start of injection can be seen in Figure 2. Phase 2 cannot be considered as cold-start because the engine temperature within this phase increased to higher than 70°C. In this phase, both the engine coolant and oil temperatures were sub-optimal and still increasing.

Phase 3 had higher PN compared to Phase 1. The increase was between 11 to 55% with different fuels. For example, with D80C20, the PN concentration increased by 11%, with D100, PN increased by 55%. Within this phase, the engine coolant temperature was optimal. However, this phase cannot be considered as hot-operation (stable operation) given that within this phase the engine oil temperature was sub-optimal and still increasing. Comparing this to Phase 2, within this phase, the start of injection stayed constant and did not change until the end of the test.

Phase 4 can be considered as hot-operation given that within this phase, the engine load/speed and the start of injection stayed constant, and also the engine oil and coolant temperatures were optimal. Phase 4 shows that the PN concentration during this hot-operation phase was higher than cold-start (Phase 1). The range of increase with different fuels was from 10 to 52%. For example, with D100, the PN concertation was 52% higher than Phase 1, with D80C20, the PN concentration was 11% higher. It can also be seen that, for all of the fuels, the PN concentration in Phase 3 is slightly higher than Phase 4 (~2%). The difference between Phase 3 and Phase 4 shows the effect of sub-optimal oil temperature when the coolant temperature is optimal.

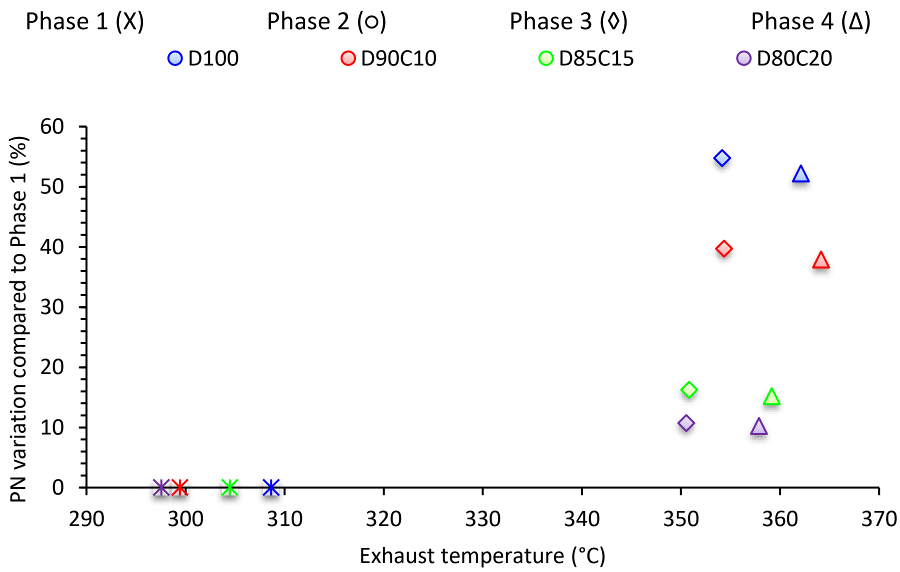

Figure 5 PN variation compared to Phase 1 vs. exhaust gas temperature at different phases with all the tested fuels

The main contributors to PN emissions are nanoparticles [28]. Figure 6 shows that for each fuel, compared to Phase 1, the median diameter increased significantly in Phase 2 and then decreased in Phases 3 and 4. It is reported in the literature that increased exhaust gas temperature is associated with an increase in nanoparticles [65]. This can be seen in Figure 7, where for each fuel from Phase 2 to Phase 4 the increased exhaust temperature is associated with a decreased median diameter. This can also be seen in Figure 7 where moving from Phase 2 to Phase 4 is associated with an increased number of nanoparticles.

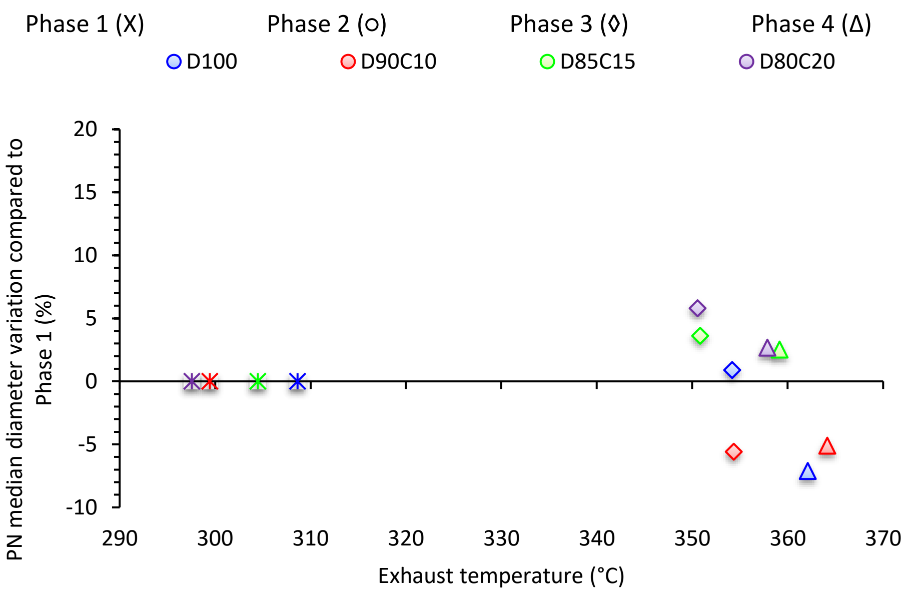

Figure 6 Median diameter variation compared to Phase 1 vs. exhaust gas temperature at different phases with all the tested fuels

Figure 7 shows the PN and PM size distribution at the four phases of engine warm-up. In this study, particles are categorised into nucleation (5-50 nm) or accumulation modes (50-500 nm) [28]. Nucleation mode particles, which contribute negligibly to PM, but significantly to PN, are predominately volatile organic compounds (VOCs) and sulfur compounds—formed within dilution and sampling—and also metal compounds and solid carbons—formed during the combustion process [28]. In Figure 7, comparing the PN and PM size distribution graphs for each fuel at each phase, which are shown with the same colour but two different shapes (○ and Δ) in each sub-figure, shows that for the size range of 5 to 50 nm in which the number of particles was significantly high, the mass of particles was low. This can be better observed in Figure 8 where the cumulative share of PN and PM at different size ranges is presented. As can be seen, for all of the fuels at all the phases, the cumulative share of sub-50 nm particles was between 0.3 to 0.9% of the total mass, while depending on the phase/fuel 11 to 29% of the total PN were related to sub-50 nm. Also, depending on phase/fuel, for the sub-30 and sub-23 nm particles, the PM cumulative share were up to 0.06 and 0.02%; while, their cumulative PN share were 13 and 9%, respectively. Therefore, excluding sub-23 nm particles in the current regulation means neglecting a significantly high number of small and toxic particles, considering the number of vehicles in cities and the PN limit in the emissions standards (e.g. 6x10^11 #/km in Euro 6 and WLTP).

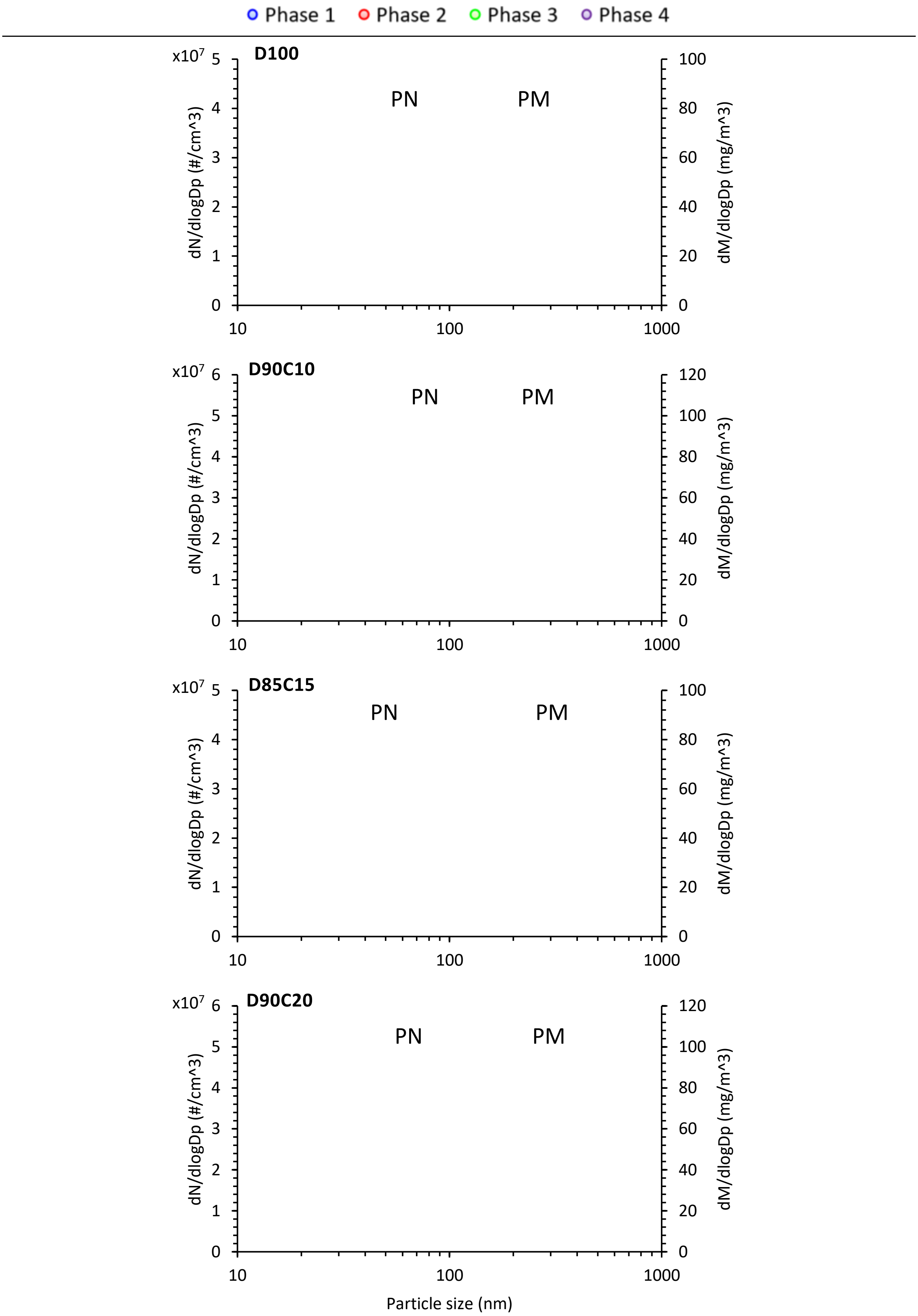

Figure 7 PN and PM size distribution at different phases with all the tested fuels

The main contributor to the accumulation mode particles are carbonaceous agglomerates and adsorb materials [28]. The agglomeration of particles in the nucleation mode by the condensation of volatile materials can also form some particles in the accumulation mode [28]. Figure 8 shows that sub-100 nm particles contributed to 53-67% of PN while only to 8-14% of PM. 92-96% of PN was related to sub-200 nm, while only 50-66% of the total mass was related to these particles. It can be seen that in the accumulation mode, the share of PN decreased as the share of PM increased. Comparing PN and PM size distribution graphs in Figure 7 shows that the contribution of particles above 50 nm to PM was significant. This is more significant for the sizes above 100 nm where the share of PN was decreasing. This can be better explained by comparing Figure 9, which shows the PM median diameter, with Figure 4, which shows the PN median diameter. It can be seen that the PM median diameter was between 173 to 213 nm, while for PN the median diameter changed between 79 to 100 nm. This can clearly show that accumulation particles have a major contribution to PM. The PN and PM size distribution in each phase are different and need to be further investigated.

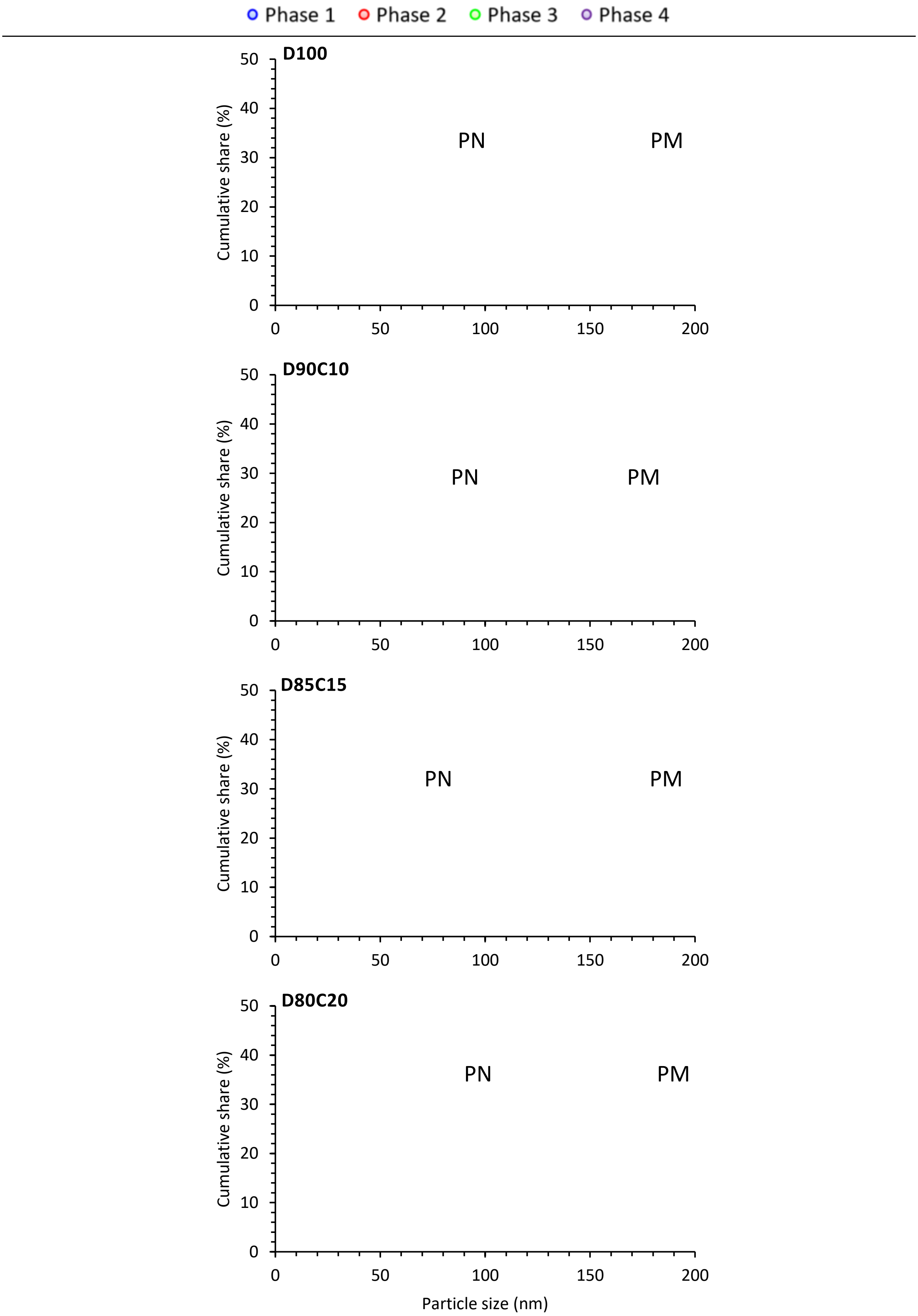

433 Figure 8 Cumulative PN and PM share at different phases with all of the tested fuels

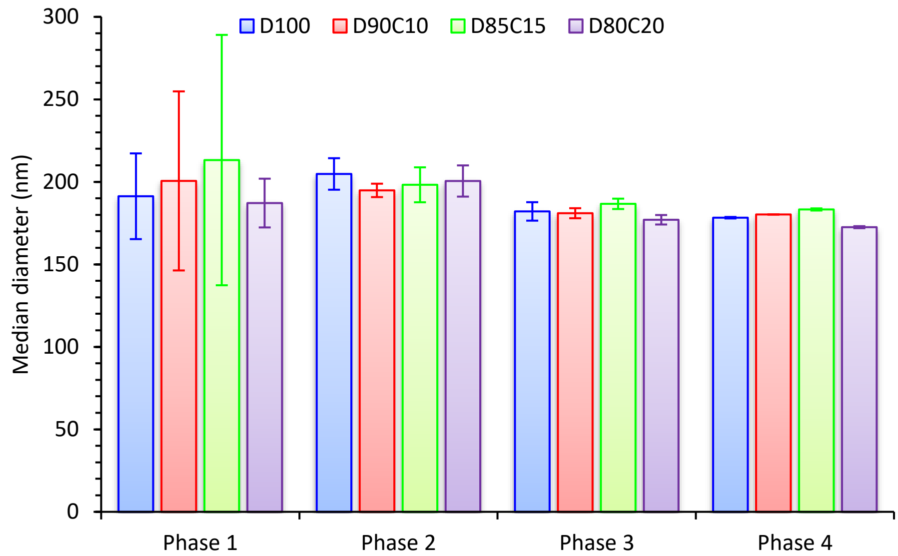

Figure 9 PM median diameter at different phases with all of the tested fuels

A decrease in the size of particles can indicate a higher share of nucleation mode. The median diameter trend observed in Figure 4 reflects the trend of PN share in the nucleation mode in Figure 8. The median diameter of the particles increases from Phase 1 to Phase 2 (because of the change in injection strategy) and decreases gradually through the engine warm-up period. Therefore, an inverse trend can be seen for the share of nucleation mode particles where the cumulative PN share of sub-50 nm and sub-23 nm particles decreased from Phase 1 to Phase 2 and then increases gradually.

Figure 4 showed that within Phase 1, which is the formal cold-start period, the PN median diameter with different fuels was between 79 to 94 nm. Figure 6 also showed how the median diameter changed through different phases as the engine exhaust temperature increased. Figure 8 shows that in Phase 1, with different fuels, between 19 to 29% of PN and less than 0.8% of PM are in the nucleation mode (5-50 nm). Out of that, the share of sub-23 nm was between 1 to 9% for PN and less than 0.02% for PM. During cold-start (Phase 1), the low temperature of the exhaust pipe can decrease the exhaust gas temperature and within this cooling process, the volatile materials can nucleate homogeneously into particles [66]. The reason for this is that a decrease in the exhaust gas temperature increases the saturation vapour pressure and saturation ratio of the volatile materials, which can lead to nucleation and condensation of volatile materials [67]. It is reported that VOCs during cold-start are higher than hot-start [68], therefore there is a high chance of nucleation. This is more significant with biofuel blends owing to their higher VOCs compared to diesel [69].

Figure 7 shows that in Phase 2, the particle size distribution graph tends toward higher PN and also bigger particles when compared to Phase 1. This can be better seen in Figure 6 where the median diameter of particles increased from Phase 1 to Phase 2. As an example, the PN median diameter increased from 86 nm to 99 nm with D100. The increase in median diameter from Phase 1 to Phase 2 was between 7 to 15%. Moving toward bigger particles in Phase 2 can also be seen by comparing the red colour to the blue colour in Figure 7 and in Figure 8 where the cumulative share of PN in the nucleation mode decreased significantly in Phase 2 compared to Phase 1. For example, with D100, the share of nucleation mode particles decreased from 20% to 12%, with D85C15 the decrease was from 30 to 20%. The share of sub-23 nm particles also decreased in Phase 2. The reason for this move toward bigger particles can be due to the injection strategy change within this unsteady warm-up phase in which the start of injection increased significantly and led to decreased ignition delay adversely affecting fuel atomisation and premixed combustion. The other variable between Phases 1 and 2 was the engine temperature, however, this parameter might not be the reason for the increased diameter size. The observed trend in Figure 6 showed that increasing the engine temperature can lead to a decrease in the size of particles. The decreasing trend of median diameter between Phase 2 to Phase 4 in Figure 6 can show that.

In Phase 3, particles were smaller than Phase 2, however, they are still bigger than Phase 1 (with most of the fuels). This can be seen in Figure 6 and Figure 7. In this phase, the median diameter of the particles with different fuels was mostly between 82 to 88 nm (Figure 4). In this phase, the start of injection stayed constant, however, the engine temperature—presented by exhaust temperature—was still increasing. Comparing Phase 3 to Phase 2, Figure 6 shows that the increasing trend of exhaust temperature is associated with a decrease in median diameter. This can also be seen in Figure 8 where the share of nucleation mode particles increased compared to Phase 2. For example, with D100, the sub-50 nm particle share increased from 12 to 18% and from 14 to 17% with D85C15. Also, in this phase, the share of sub-23 nm particles increased.

Comparing Phase 4 to Phase 3 and Phase 2 shows that the increased exhaust temperature is associated with a decrease in particle size. This decreasing trend between the median diameter and exhaust temperature can be seen in Figure 6. It can also be seen in Figure 8 that the share of nucleation mode particles in Phase 4 was higher than Phase 3. This can be due to the effect of sub-optimal engine oil temperature. However, the change was small with most of the fuels. For example, with D80C20, the nucleation mode particles increased from 17 to 18%. Comparing Phase 4 to Phase 1 shows a different trend with different fuels, which means that the fuel properties are likely to be the driving factor.

3.2 Effect of fuel

Figure 3 showed that the PN concentration increased in all of the phases when the fuel blends were used instead of diesel. For example, using D90C10 increased PN by 27, 36, 15 and 15% from Phase 1 to 4, respectively. The reason for this can be the higher volatile organic compounds (VOCs) of biofuels when compared to diesel [69]. It was also observed in Figure 5 that compared to D100, these fuels showed less difference between cold-start and hot-operation. Comparing Phase 3 and 4 to Phase 1, in Figure 5, shows that the PN variation decreased by increasing the share of biofuel in the blend. For example, with D100, D90C10, D85C15 and D80C20, PN during Phase 4 was 52, 38, 15 and 10% higher than Phase 1. However, this can be misleading, and the data can be evaluated from another aspect. Figure 10 shows how the PN concentration changed with different fuels compared to D100. It can be seen that using D90C10, D85C15 and D80C20, instead of D100, increased the PN concentration in all of the phases. However, the increase was more significant during cold-start. For example, in Phase 1, which is cold-start, using these fuels instead of D100 increased PN between 27 to 57%; while, during hot-operation the increase range was between 4 to 19%. This is an important observation because using these fuels has more adverse impacts within the cold-start period, which is an inevitable part of daily driving for most vehicles. This analysis shows that the evaluation of using such fuels needs to be done not only during hot-operation, but also cold-start. A reason for the increased PN with the fuel blends during cold-start could be the higher viscosity of biofuels, which adversely affects fuel atomisation and evaporation [70]. Another reason could be the increased number of small particles. The higher oxygen content of biofuels can also result in higher PN. In biofuels, there is more oxygen available in the center of the diffusion flame (where usually the concentration of HC is higher). This could result in smaller primary particle diameters and an increase of smaller size particles.

The adverse effect of using biofuels can be further highlighted in Figure 11, where the PN median diameter with these fuels during the first two phases is smaller than D100 (in most of the cases); while during Phase 4, D100 has the lowest median diameter. This means that these fuels emit smaller particles during cold-start. This is important as a decrease in particle size has been shown to be associated with an increase in toxicity [33].

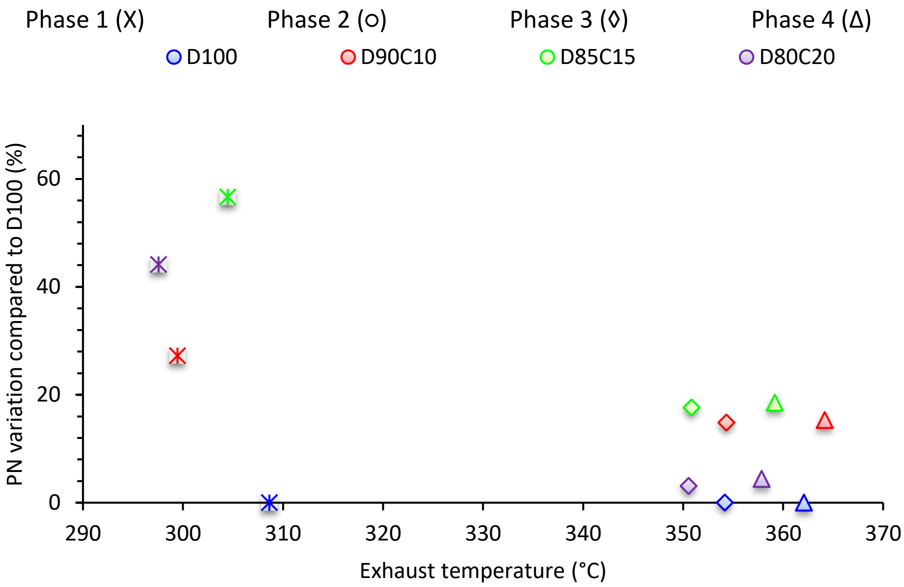

Figure 10 PN variation compared to D100 vs. exhaust gas temperature at different phases with all of the tested fuels

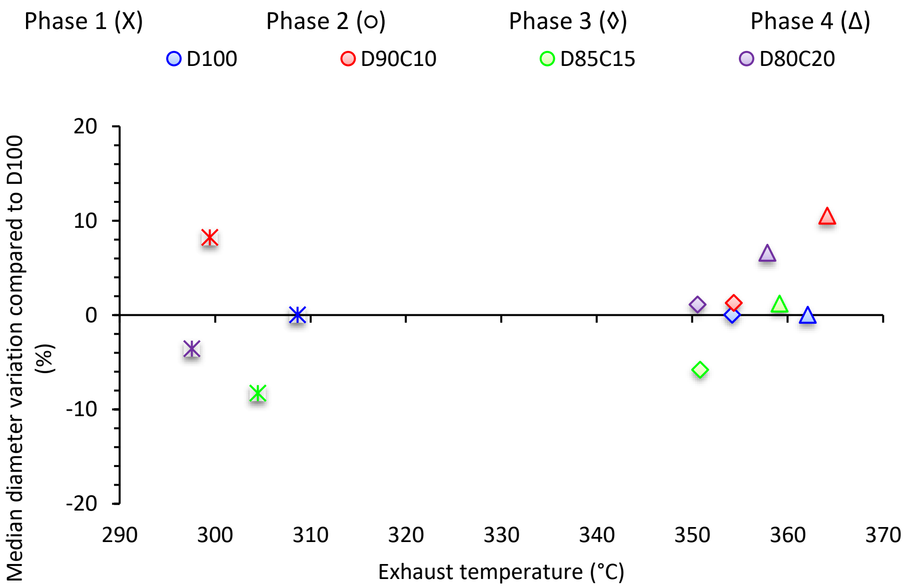

Figure 11 Median diameter variation compared to D100 vs. exhaust gas temperature at different phases

The increase in smaller particles is shown in Figure 12 which shows the cumulative share of nucleation mode particles at different phases. Figure 12 shows that during cold-start the share of nucleation mode particles increased significantly when D100 was replaced by the fuel blends. For example, the share of sub-50 nm particles with D100, D90C10, D85C15 and D80C20 were 20, 20, 29 and 23% in Phase 1, and 12, 12, 20 and 14% in Phase 2, respectively. A similar trend was also observed for sub-23 nm particles. For example, the share of these particles in Phase 1 increased from 1 to 9% when D100 was replaced with D85C15.

It was mentioned that nucleation mode particles (sub-50 nm) are mainly volatile organic compounds (VOCs), sulfur compounds, metal compounds and solid carbons [28]. It is known that biofuels have higher VOCs compared to diesel [69], therefore the higher VOCs of the tested fuels compared to D100 could be the reason for the increased share of nucleation mode particles and therefore the total PN. A greater amount of VOCs with biofuel was also reported by Hedayat et al. [71], which used the same type of engine as this study, under a stationary cycle.

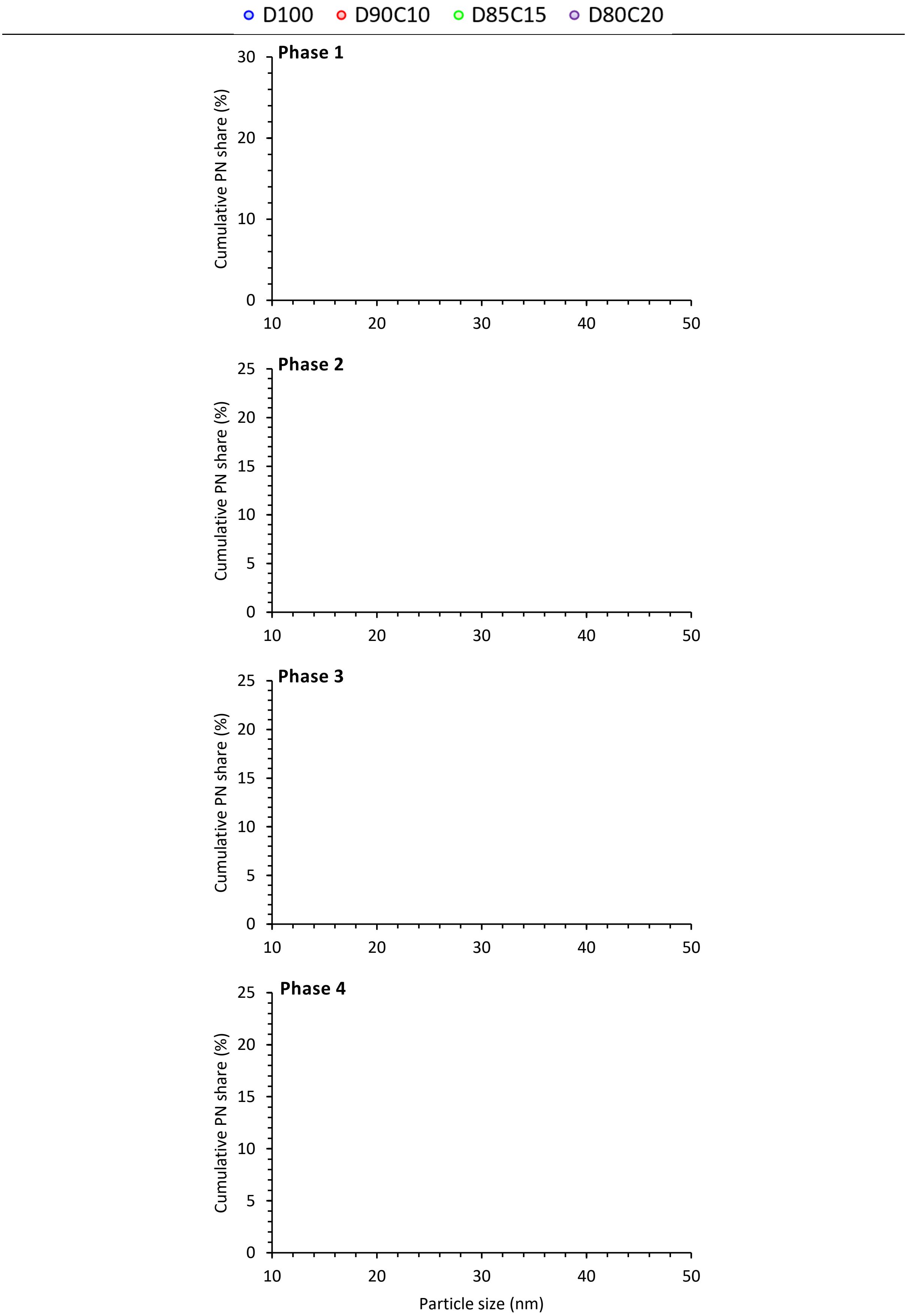

Figure 12 Cumulative PN share at different phases with all of the tested fuels

3.3 Practical implications of this study

Due to the high price and adverse health effects of fossil fuels, there is a focus to increase the use of biofuels and measures have been in place. However, vehicle emissions are still an issue and governments and authorities are trying to limit the amount of emission by tightening the emissions levels from vehicles in the emission regulations. This research is related to the future emissions regulations (Euro 7) and introduces important knowledge about regulated and currently-unregulated particulate number emissions during cold-start and engine warm-up, which is an emerging area in the literature. This study shows that when it comes to very small particles (which are more toxic), the current market trend (increasing the share of biofuel) can have a more adverse impact (because of more small particles) within the cold-start period—which is inevitable in most vehicles' daily driving schedule. But, even the latest emission regulations, such as WLTP, only consider particles with a size above 23 nm. Most cold-start operations occur in residential areas, and this study shows that a significant portion of emitted particles are smaller than 23 nm during cold-start, and also the current fuel market leads to an even higher number of these small particles. And the current regulations do not include a practical enough measure to limit such emissions. Including sub-23 nm particles in regulations (through PMP) increases the number of particles measured during the homologation tests, and this might lead many vehicles to fail to comply with the PN limit in emissions certification tests. However, passing or failing the certification test does not change the fact that these days many certified vehicles on the street are emitting a huge number of small particles affecting people's health and still the emission regulations are unable to stop them. This study emphasizes the importance of including smaller (sub-23 nm) particles in future regulations, or even in the new amendments of the current regulations.

4. Conclusions

Using a diesel engine fueled by diesel and biofuels, this research evaluated PN, PN and PM median diameter, PN and PM size distribution, the share of particles at different sizes including nucleation mode and sub-23 nm particles. This research divided the engine warm-up period into four phases of cold-start (Phase 1) to hot-operation (Phase 4) and two intermediate unsteady warm-up phases which could be counted neither as cold-start (defined in the regulations) nor as hot-operation.

Results showed that for all of the fuels, compared to Phase 1, PN increased by 27-39% in Phase 2, 11-55% in Phase 3 and 10-52% in Phase 4. In the cold-start phase, between 19 to 29% of the total PN and less than 0.8% of the total PM were related to particles in the nucleation mode (sub-50 nm). Out of that, the share of sub-23 nm was between 1 to 9% for PN and less than 0.02% for PM. By using biofuel blends instead of diesel, PN increased between 27 to 57% during cold-start; while, during hot-operation, the increase in PN ranged between 4 to 19%. Also, the PN median diameter decreased during the first two phases and nucleation mode particles increased significantly. For all of the fuels at the different phases, the PM median diameter was between 173 to 213 nm, while for PN the median diameter was between 79 to 100 nm. The cumulative share of sub-50 nm particles was 0.3-0.9% of the total mass, while 11-29% of the total PN. For the sub-30 and sub-23 nm particles, the PM cumulative share was up to 0.06 and 0.02%; while, their PN cumulative share was 13 and 9%, respectively. The contribution of particles above 50 nm to PM was significantly high. This was more significant for the sizes above 100 nm where the share of PN was decreasing. Sub-100 nm particles contributed to 53-67% of PN while only to 8-14% of PM. 92-96% of PN was related to sub-200 nm, while only 50-66% of the total mass was related to this size range. In the accumulation mode, the share of PN decreased as the share of PM increased.

5. Acknowledgement

The authors would like to acknowledge the support of Australian Research Council Linkage Projects funding scheme (project number LP110200158), Prof. Jochen Mueller, Mr. Andrew Elder and Mr. Noel Hartnett for their assistance.

6. References

1. Joshi, A., *Review of Vehicle Engine Efficiency and Emissions.* SAE International Journal of Engines, 2020. 10.4271/2020-01-0352.
2. Verma, T.N., P. Nashine, P.K. Chaurasiya, U. Rajak, A. Afzal, S. Kumar, D.V. Singh and A.K. Azad, *The effect of ethanol-methanol-diesel-microalgae blends on performance, combustion and emissions of a direct injection diesel engine.* Sustainable Energy Technologies and Assessments, 2020. **42**: p. 100851. https://doi.org/10.1016/j.seta.2020.100851.
3. Sathyamurthy, R., D. Balaji, S. Gorjian, S.J. Muthiya, R. Bharathwaaj, S. Vasanthaseelan and F.A. Essa, *Performance, combustion and emission characteristics of a DI-CI diesel engine fueled with corn oil methyl ester biodiesel blends.* Sustainable Energy Technologies and Assessments, 2021. **43**: p. 100981. https://doi.org/10.1016/j.seta.2020.100981.
4. Abrar, I. and A.N. Bhaskarwar, *Performance and emission characteristics of constant speed diesel engine fueled by surfactant-free microemulsions.* Sustainable Energy Technologies and Assessments, 2021. **47**: p. 101414. https://doi.org/10.1016/j.seta.2021.101414.
5. Elkelawy, M., A.E. Kabeel, E.A. El Shenawy, H. Panchal, A. Elbanna, H.A.-E. Bastawissi and K.K. Sadasivuni, *Experimental investigation on the influences of acetone organic compound additives into the diesel/biodiesel mixture in CI engine.* Sustainable Energy Technologies and Assessments, 2020. **37**: p. 100614. https://doi.org/10.1016/j.seta.2019.100614.
6. Nabi, M.N., A. Zare, F.M. Hossain, T.A. Bodisco, Z.D. Ristovski and R.J. Brown, *A parametric study on engine performance and emissions with neat diesel and diesel-butanol blends in the 13-Mode European Stationary Cycle.* Energy Conversion and Management, 2017. **148**: p. 251-259. https://doi.org/10.1016/j.enconman.2017.06.001.
7. Verma, T.N., P. Shrivastava, U. Rajak, G. Dwivedi, S. Jain, A. Zare, A.K. Shukla and P. Verma, *A comprehensive review of the influence of physicochemical properties of biodiesel on combustion characteristics, engine performance and emissions.* Journal of Traffic and Transportation Engineering (English Edition), 2021. **8**(4): p. 510-533. https://doi.org/10.1016/j.jtte.2021.04.006.
8. Zare, A., M.N. Nabi, T.A. Bodisco, F.M. Hossain, M.M. Rahman, Z.D. Ristovski and R.J. Brown, *The effect of triacetin as a fuel additive to waste cooking biodiesel on engine*

performance and exhaust emissions. Fuel, 2016. **182**: p. 640-649. https://doi.org/10.1016/j.fuel.2016.06.039.
9. Zare, A., R.J. Brown and T. Bodisco, *Ethanol Fumigation and Engine Performance in a Diesel Engine*, in *Alcohol as an Alternative Fuel for Internal Combustion Engines*. 2021, Springer. p. 191-212.
10. Nabi, M.N., A. Zare, F.M. Hossain, M.M. Rahman, T.A. Bodisco, Z.D. Ristovski and R.J. Brown, *Influence of fuel-borne oxygen on European Stationary Cycle: Diesel engine performance and emissions with a special emphasis on particulate and NO emissions.* Energy Conversion and Management, 2016. **127**: p. 187-198. https://doi.org/10.1016/j.enconman.2016.09.010.
11. Zare, A., T.A. Bodisco, M.N. Nabi, F.M. Hossain, Z.D. Ristovski and R.J. Brown, *Engine Performance during Transient and Steady-State Operation with Oxygenated Fuels.* Energy & Fuels, 2017. **31**(7): p. 7510-7522. 10.1021/acs.energyfuels.7b00429.
12. Nabi, M.N., A. Zare, F.M. Hossain, Z.D. Ristovski and R.J. Brown, *Reductions in diesel emissions including PM and PN emissions with diesel-biodiesel blends.* Journal of Cleaner Production, 2017. **166**: p. 860-868. https://doi.org/10.1016/j.jclepro.2017.08.096.
13. Bencheikh, K., A.E. Atabani, S. Shobana, M.N. Mohammed, G. Uğuz, O. Arpa, G. Kumar, A. Ayanoğlu and A. Bokhari, *Fuels properties, characterizations and engine and emission performance analyses of ternary waste cooking oil biodiesel–diesel–propanol blends.* Sustainable Energy Technologies and Assessments, 2019. **35**: p. 321-334. https://doi.org/10.1016/j.seta.2019.08.007.
14. Attia, A.M.A., M. Nour, A.I. El-Seesy and S.A. Nada, *The effect of castor oil methyl ester blending ratio on the environmental and the combustion characteristics of diesel engine under standard testing conditions.* Sustainable Energy Technologies and Assessments, 2020. **42**: p. 100843. https://doi.org/10.1016/j.seta.2020.100843.
15. Lapuerta, M., O. Armas and J. Rodríguez-Fernández, *Effect of biodiesel fuels on diesel engine emissions.* Progress in Energy and Combustion Science, 2008. **34**(2): p. 198-223. https://doi.org/10.1016/j.pecs.2007.07.001.
16. de Morais, A.M., S. de Morais Hanriot, A. de Oliveira, M.A.M. Justino, O.S. Valente and J.R. Sodré, *An assessment of fuel consumption and emissions from a diesel power generator converted to operate with ethanol.* Sustainable Energy Technologies and Assessments, 2019. **35**: p. 291-297. https://doi.org/10.1016/j.seta.2019.08.005.
17. Singh, G., A.P. Singh and A.K. Agarwal, *Experimental investigations of combustion, performance and emission characterization of biodiesel fuelled HCCI engine using external mixture formation technique.* Sustainable Energy Technologies and Assessments, 2014. **6**: p. 116-128. https://doi.org/10.1016/j.seta.2014.01.002.
18. Giakoumis, E.G., C.D. Rakopoulos, A.M. Dimaratos and D.C. Rakopoulos, *Exhaust emissions of diesel engines operating under transient conditions with biodiesel fuel blends.* Progress in Energy and Combustion Science, 2012. **38**(5): p. 691-715. https://doi.org/10.1016/j.pecs.2012.05.002.
19. Datta, A. and B.K. Mandal, *A comprehensive review of biodiesel as an alternative fuel for compression ignition engine.* Renewable and Sustainable Energy Reviews, 2016. **57**: p. 799-821. https://doi.org/10.1016/j.rser.2015.12.170.
20. Nabi, N., A. Zare, M. Hossain, M.M. Rahman, D. Stuart, Z. Ristovski and R. Brown. *Formulation of new oxygenated fuels and their influence on engine performance and exhaust emissions*. The Combustion Institute Australia and New Zealand Section.

21. Verma, P., S. Stevanovic, A. Zare, G. Dwivedi, T. Chu Van, M. Davidson, T. Rainey, R.J. Brown and Z.D. Ristovski, *An overview of the influence of biodiesel, alcohols, and various oxygenated additives on the particulate matter emissions from diesel engines.* Energies, 2019. **12**(10): p. 1987
22. World Health Organization, *Review of evidence on health aspects of air pollution–REVIHAAP Project.* 2013
23. Vaughan, A., S. Stevanovic, A.P. Banks, A. Zare, M.M. Rahman, R.V. Bowman, K.M. Fong, Z.D. Ristovski and I.A. Yang, *The cytotoxic, inflammatory and oxidative potential of coconut oil-substituted diesel emissions on bronchial epithelial cells at an air-liquid interface.* Environmental Science Pollution Research, 2019. **26**(27): p. 27783-27791
24. Vaughan, A., S. Stevanovic, M. Rahman, A. Zare, B. Miljevic, Z. Ristovski, R. Bowman, K. Fong and I. Yang, *N-acetyl cysteine (NAC) intervention attenuates the effects of diesel and biodiesel emission exposure on human bronchial epithelial cells, 16HBE, at air-liquid interface.* European Respiratory Journal, 2016
25. Stevanovic, S., A. Vaughan, F. Hedayat, F. Salimi, M.M. Rahman, A. Zare, R.A. Brown, R.J. Brown, H. Wang and Z. Zhang, *Oxidative potential of gas phase combustion emissions-An underestimated and potentially harmful component of air pollution from combustion processes.* Atmospheric environment, 2017. **158**: p. 227-235
26. Vaughan, A., S. Stevanovic, A. Zare, M. Rahman, B. Miljevic, Z. Ristovski, R. Bowman, K. Fong and I. Yang, *Coconut oil substitution in diesel fuel alters human bronchial epithelial cell responses to diesel emission exposure at the air–liquid interfacein vitro: to 022.* Respirology, 2016. **21**
27. Vaughan, A., S. Stevanovic, L.E. Morrison, A.M. Pourkhesalian, M.M. Rahman, A. Zare, B. Miljevic, F. Goh, V. Relan and R. Bowman, *Removal of organic content from diesel exhaust particles alters cellular responses of primary human bronchial epithelial cells cultured at an air-liquid interface.* Journal of Environmental Analytical Toxicology, 2015. **5**(5): p. 100316-1
28. Kittelson, D.B., *Engines and nanoparticles: a review.* Journal of aerosol science, 1998. **29**(5-6): p. 575–588
29. Delphi Technologies, *Worldwide emissions standards-Passenger cars and light duty vehicles.* Delphi, 2019. https://www.delphi.com/innovations.
30. Chen, L., S. Ding, H. Liu, Y. Lu, Y. Li and A.P. Roskilly, *Comparative study of combustion and emissions of kerosene (RP-3), kerosene-pentanol blends and diesel in a compression ignition engine.* Applied Energy, 2017. **203**: p. 91-100
31. Zare, A., T.A. Bodisco, M.N. Nabi, F.M. Hossain, M.M. Rahman, Z.D. Ristovski and R.J. Brown, *The influence of oxygenated fuels on transient and steady-state engine emissions.* Energy, 2017. **121**: p. 841-853. https://doi.org/10.1016/j.energy.2017.01.058.
32. Chen, L., X. Hu, J. Wang and Y. Yu, *Impacts of alternative fuels on morphological and nanostructural characteristics of soot emissions from an aviation piston engine.* Environmental science & technology, 2019. **53**(8): p. 4667-4674
33. Krahl, J., J. Bünger, O. Schröder, A. Munack and G. Knothe, *Exhaust emissions and health effects of particulate matter from agricultural tractors operating on rapeseed oil methyl ester.* Journal of the American Oil Chemists' Society, 2002. **79**(7): p. 717-724

34. Giechaskiel, B., T. Lähde, S. Gandi, S. Keller, P. Kreutziger and A. Mamakos, *Assessment of 10-nm Particle Number (PN) Portable Emissions Measurement Systems (PEMS) for Future Regulations.* International Journal of Environmental Research and Public Health, 2020. **17**(11). 10.3390/ijerph17113878.

35. Giechaskiel, B., *Effect of Sampling Conditions on the Sub-23 nm Nonvolatile Particle Emissions Measurements of a Moped.* Applied Sciences, 2019. **9**(15). 10.3390/app9153112.

36. Giechaskiel, B., T. Lähde, A.D. Melas, V. Valverde and M. Clairotte, *Uncertainty of laboratory and portable solid particle number systems for regulatory measurements of vehicle emissions.* Environmental Research, 2021. **197**: p. 111068. https://doi.org/10.1016/j.envres.2021.111068.

37. Andersson, J., A. Mamakos, Z.C. Samaras, Z. Toumasatos, A. Kontses, L.D. Ntziachristos, A. Bergmann, S. Hausberger, L. Landl, M. Bainschab, J. Keskinen and C. Haisch, *Measuring Automotive Exhaust Particles Down to 10 nm.* SAE International Journal of Advances and Current Practices in Mobility, 2020. **3**(1): p. 539-550. https://doi.org/10.4271/2020-01-2209.

38. Leach, F., A. Lewis, S. Akehurst, J. Turner and D. Richardson, *Sub-23 nm particulate emissions from a highly boosted GDI engine.* SAE Technical Paper, 2019. 0148-7191.

39. Lodi, F., A. Zare, P. Arora, S. Stevanovic, P. Verma, M. Jafari, Z. Ristovski, R. Brown and T. Bodisco, *Characteristics of Particle Number and Particle Mass Emissions of a Diesel Engine during Cold-, Warm-, and Hot-Start Operation.* SAE Technical Paper, 2021. https://doi.org/10.4271/2021-01-5061.

40. Reiter, M.S. and K.M. Kockelman, *The problem of cold starts: A closer look at mobile source emissions levels.* Transportation Research Part D: Transport and Environment, 2016. **43**: p. 123-132

41. André, M., *In actual use car testing: 70,000 kilometers and 10,000 trips by 55 French cars under real conditions.* SAE transactions, 1991: p. 65-72

42. Zare, A., S. Stevanovic, M. Jafari, P. Verma, M. Babaie, L. Yang, M.M. Rahman, Z.D. Ristovski, R.J. Brown and T.A. Bodisco, *Analysis of cold-start NO2 and NOx emissions, and the NO2/NOx ratio in a diesel engine powered with different diesel-biodiesel blends.* Environmental Pollution, 2021. **290**: p. 118052. https://doi.org/10.1016/j.envpol.2021.118052.

43. Shi, Z., C.-f. Lee, H. Wu, Y. Wu, L. Zhang and F. Liu, *Optical diagnostics of low-temperature ignition and combustion characteristics of diesel/kerosene blends under cold-start conditions.* Applied Energy, 2019. **251**: p. 113307. https://doi.org/10.1016/j.apenergy.2019.113307.

44. Lodi, F., A. Zare, P. Arora, S. Stevanovic, M. Jafari, Z. Ristovski, R.J. Brown and T. Bodisco, *Combustion Analysis of a Diesel Engine during Warm up at Different Coolant and Lubricating Oil Temperatures.* Energies, 2020. **13**(15): p. 3931

45. Verma, P., M. Jafari, A. Zare, E. Pickering, Y. Guo, C.G. Osuagwu, S. Stevanovic, R. Brown and Z. Ristovski, *Soot particle morphology and nanostructure with oxygenated fuels: A comparative study into cold-start and hot-start operation.* Environmental Pollution, 2021. **275**: p. 116592. https://doi.org/10.1016/j.envpol.2021.116592.

46. Zare, A., T.A. Bodisco, M.N. Nabi, F.M. Hossain, Z.D. Ristovski and R.J. Brown, *A comparative investigation into cold-start and hot-start operation of diesel engine performance with oxygenated fuels during transient and steady-state operation.* Fuel, 2018. **228**: p. 390-404. https://doi.org/10.1016/j.fuel.2018.05.004.

47. Zare, A., M.N. Nabi, T.A. Bodisco, F.M. Hossain, M.M. Rahman, T. Chu Van, Z.D. Ristovski and R.J. Brown, *Diesel engine emissions with oxygenated fuels: A comparative study into cold-start and hot-start operation.* Journal of Cleaner Production, 2017. **162**: p. 997-1008. https://doi.org/10.1016/j.jclepro.2017.06.052.
48. Lodi, F., A. Zare, P. Arora, S. Stevanovic, M. Jafari, Z. Ristovski, R.J. Brown and T. Bodisco, *Engine Performance and Emissions Analysis in a Cold, Intermediate and Hot Start Diesel Engine.* Applied Sciences, 2020. **10**(11): p. 3839
49. Nam, E., *Analysis of particulate matter emissions from light-duty gasoline vehicles in Kansas City*. 2008: US Environmental Protection Agency.
50. Lee, D.-W., J. Johnson, J. Lv, K. Novak and J. Zietsman, *Comparisons between vehicular emissions from real-world in-use testing and EPA moves estimation.* Texas Transportation Institute, 2012.
51. Roberts, A., R. Brooks and P. Shipway, *Internal combustion engine cold-start efficiency: A review of the problem, causes and potential solutions.* Energy Conversion and Management, 2014. **82**: p. 327-350
52. Zare, A., T.A. Bodisco, P. Verma, M. Jafari, M. Babaie, L. Yang, M.M. Rahman, A. Banks, Z.D. Ristovski and R.J. Brown, *Emissions and performance with diesel and waste lubricating oil: A fundamental study into cold start operation with a special focus on particle number size distribution.* Energy Conversion and Management, 2020. **209**: p. 112604
53. Bodisco, T. and R.J. Brown, *Inter-cycle variability of in-cylinder pressure parameters in an ethanol fumigated common rail diesel engine.* Energy, 2013. **52**: p. 55-65
54. Bodisco, T., P. Tröndle and R.J. Brown, *Inter-cycle variability of ignition delay in an ethanol fumigated common rail diesel engine.* Energy, 2015. **84**: p. 186-195
55. Su, S., T. Lv, Y. Lai, J. Mu, Y. Ge and B. Giechaskiel, *Particulate emissions of heavy duty diesel engines measured from the tailpipe and the dilution tunnel.* Journal of Aerosol Science, 2021. **156**: p. 105799. https://doi.org/10.1016/j.jaerosci.2021.105799.
56. Giechaskiel, B., A.D. Melas, T. Lähde and G. Martini, *Non-Volatile Particle Number Emission Measurements with Catalytic Strippers: A Review.* Vehicles, 2020. **2**(2). 10.3390/vehicles2020019.
57. TSI, *Aerosol Instrument Manager® Software for Scanning Mobility Particle Sizer™ (SMPS™) Spectrometer*. 2010, TSI. p. 71.
58. Giakoumis, E.G., C.D. Rakopoulos and D.C. Rakopoulos, *Assessment of NOx Emissions during Transient Diesel Engine Operation with Biodiesel Blends.* Journal of Energy Engineering 2014. **140**(3): p. A4014004. doi:10.1061/(ASCE)EY.1943-7897.0000136.
59. Van, T.C., A. Zare, M. Jafari, T.A. Bodisco, N. Surawski, P. Verma, K. Suara, Z. Ristovski, T. Rainey and S. Stevanovic, *Effect of cold start on engine performance and emissions from diesel engines using IMO-Compliant distillate fuels.* Environmental Pollution, 2019. **255**: p. 113260
60. Mitchell, B.J., A. Zare, T.A. Bodisco, M.N. Nabi, F.M. Hossain, Z.D. Ristovski and R.J. Brown, *Engine blow-by with oxygenated fuels: A comparative study into cold and hot start operation.* Energy, 2017. **140**: p. 612-624
61. Zare, A., T.A. Bodisco, M. Jafari, P. Verma, L. Yang, M. Babaie, M.M. Rahman, A. Banks, Z.D. Ristovski, R.J. Brown and S. Stevanovic, *Cold-start NOx emissions: Diesel and waste lubricating oil as a fuel additive.* Fuel, 2021. **286**: p. 119430. https://doi.org/10.1016/j.fuel.2020.119430.

62. Chien, S.-M., Y.-J. Huang, S.-C. Chuang and H.-H. Yang, *Effects of biodiesel blending on particulate and polycyclic aromatic hydrocarbon emissions in nano/ultrafine/fine/coarse ranges from diesel engine.* Aerosol and Air Quality Research, 2016. **9**(1): p. 18-31
63. Jafari, M., P. Verma, T.A. Bodisco, A. Zare, N.C. Surawski, P. Borghesani, S. Stevanovic, Y. Guo, J. Alroe, C. Osuagwu, A. Milic, B. Miljevic, Z.D. Ristovski and R.J. Brown, *Multivariate analysis of performance and emission parameters in a diesel engine using biodiesel and oxygenated additive.* Energy Conversion and Management, 2019. **201**: p. 112183. https://doi.org/10.1016/j.enconman.2019.112183.
64. Yusuf, A.A. and F.L. Inambao, *Effect of cold start emissions from gasoline-fueled engines of light-duty vehicles at low and high ambient temperatures: Recent trends.* Case Studies in Thermal Engineering, 2019. **14**: p. 100417. https://doi.org/10.1016/j.csite.2019.100417.
65. Kittelson, D.B., W.F. Watts, J.P. Johnson, C. Thorne, C. Higham, M. Payne, S. Goodier, C. Warrens, H. Preston and U. Zink, *Effect of fuel and lube oil sulfur on the performance of a diesel exhaust gas continuously regenerating trap.* Environmental science & technology, 2008. **42**(24): p. 9276-9282
66. Ning, Z., C.S. Cheung and S.X. Liu, *Experimental investigation of the effect of exhaust gas cooling on diesel particulate.* Journal of Aerosol Science, 2004. **35**(3): p. 333-345
67. Kasper, M., *Sampling and measurement of nanoparticle emissions for type approval and field control.* SAE Technical Paper, 2005. 0148-7191.
68. Tsai, J.-H., S.-Y. Chang and H.-L. Chiang, *Volatile organic compounds from the exhaust of light-duty diesel vehicles.* Atmospheric environment, 2012. **61**: p. 499-506
69. Pourkhesalian, A.M., S. Stevanovic, F. Salimi, M.M. Rahman, H. Wang, P.X. Pham, S.E. Bottle, A.R. Masri, R.J. Brown and Z.D. Ristovski, *Influence of fuel molecular structure on the volatility and oxidative potential of biodiesel particulate matter.* Environmental science & technology, 2014. **48**(21): p. 12577-12585
70. Armas, O., J.J. Hernández and M.D. Cárdenas, *Reduction of diesel smoke opacity from vegetable oil methyl esters during transient operation.* Fuel, 2006. **85**(17-18): p. 2427-2438
71. Hedayat, F., S. Stevanovic, A. Milic, B. Miljevic, M.N. Nabi, A. Zare, S.E. Bottle, R.J. Brown and Z.D. Ristovski, *Influence of oxygen content of the certain types of biodiesels on particulate oxidative potential.* Science of The Total Environment, 2016. **545-546**: p. 381-388. https://doi.org/10.1016/j.scitotenv.2015.12.036.

7. Appendix A

Table A1 shows the accuracy of the measuring instruments.

Table A1 Instrument accuracy

Instrument	Accuracy
Kistler 6053CC60 piezoelectric transducer	≈ -20 pC/bar
Kistler type 2614	0.5 crank angle degrees
CAI-600 NDIR CO_2 analyser	Linearity > 0.5% and repeatability > 1% of full scale
SABLE CA-10 Carbon CO_2 gas analyser	1% of reading within the range of 0-10%
Dynamometer	±0.5%

Table A2 shows the statistical analysis of the test repeatability for cold-start and warm-start tests with diesel using average and coefficient of variation (CoV) of engine speed and torque. As can be seen, the difference between the tests is indicating the repeatability of the experiment. In addition to these two important parameters, Table A3 shows the CO_2 repeatability. This experimental study used a non-dispersive infrared CAI-600 CO2 gas analyser which is a piece of high-tech quality equipment in the market used by different car industries and research groups to check the CO_2 emission and confirm the test repeatability. It is worth to mention that using a correlation car/engine and measuring CO_2 in the repeated tests and then calculating the variation between the correlation tests is a very common and trustworthy method of uncertainty measurement and test repeatability check in emissions laboratories of the automotive industries.

Table A2 Test repeatability: statistical analysis

		Engine speed (rpm)		Engine torque (Nm)	
		Mean	CoV (%)	Mean	CoV (%)
Warm-start	Test I	1499.49	0.14	242.02	1.00
	Test II	1498.94	0.15	238.28	1.34
	Difference	0.04%		1.5%	
Cold-start	Test I	1499.19	0.13	227.20	5.42
	Test II	1498.87	0.15	225.28	3.74
	Difference	0.02%		0.82%	

Table A3 Test repeatability: CO_2 correlation test

		Mean	CoV (%)
Warm-start	Test I	6.64	0.36
	Test II	6.47	0.51
	Difference	0.17%	
Cold-start	Test I	6.51	2.27
	Test II	6.36	0.97
	Difference	0.12%	